DALTON
FULL PAPER

Characterisation of the tetrahalophosphonium cations $PBr_nI_{4-n}^+$ ($0 \le n \le 4$) by ^{31}P MAS NMR, IR and Raman spectroscopy and the crystal structures of $PI_4^+AlCl_4^-$, $PI_4^+AlBr_4^-$ and $PI_4^+GaI_4^-$

Christoph Aubauer,[a] Martin Kaupp,[b] Thomas M. Klapötke,*[a] Heinrich Nöth,†[a] Holger Piotrowski,†[a] Wolfgang Schnick,[a] Jürgen Senker *[a] and Max Suter †[a]

[a] *Department of Chemistry, Ludwig-Maximilians-University, Butenandtstr. 5-13 (D), D-81377 Munich, Germany. E-mail: tmk@cup.uni-muenchen.de*
[b] *Institute of Inorganic Chemistry, University of Würzburg, Am Hubland, D-97074 Würzburg, Germany*

Received 6th February 2001, Accepted 12th April 2001
First published as an Advance Article on the web 18th May 2001

The novel tetrahalophosphonium salts $PBr_4^+AsF_6^-$, $PI_4^+AlCl_4^-$ and $PI_4^+EBr_4^-$ (E = Al, Ga) have been synthesised. A variety of solid complexes containing PBr_4^+ (*e.g.* $PBr_4^+AsF_6^-$, $PBr_4^+AlBr_4^-$ $PBr_4^+GaBr_4^-$), PI_4^+ (*e.g.* $PI_4^+AlCl_4^-$, $PI_4^+AlBr_4^-$, $PI_4^+GaBr_4^-$) or the mixed species $PBr_nI_{4-n}^+$ ($0 \le n \le 4$, containing $AlBr_4^-$, $GaBr_4^-$, AsF_6^- or SbF_6^-) have been studied by solid-state ^{31}P MAS NMR and vibrational spectroscopy. The influence of the counter-ion on the chemical shift and the vibrational frequencies are discussed. The crystal structures of $PI_4^+AlCl_4^-$, $PI_4^+AlBr_4^-$ and $PI_4^+GaI_4^-$ are reported. Evidence for the existence of the hitherto unknown mixed bromoiodophosphonium cations PBr_3I^+, $PBr_2I_2^+$ and $PBrI_3^+$ has been confirmed by spin–orbit corrected density functional calculations of isotropic ^{31}P chemical shifts for $PBr_nI_{4-n}^+$.

Introduction

The binary tetrahalophosphonium cations PF_4^+,[1] PCl_4^+,[2,3] PBr_4^+[2a,3,4] and PI_4^+[5–7] have been known for some time and were characterised by vibrational and ^{31}P NMR spectroscopic studies. Additionally, several crystal structure determinations have been reported for PCl_4^+ compounds with a large variation of the counter-ion.[2a,8] PBr_4^+ and PI_4^+ have been characterised only by X-ray crystallography in the salts $PBr_4^+Br^-$,[9] $PBr_4^+Br_3^-$[10] and $PI_4^+AlI_4^-$.[11]

Recently,[6] we showed in a combined theoretical and experimental study, that the PI_4^+ cation has an extremely large negative ^{31}P chemical shift in the compounds $PI_4^+AsF_6^-$ ($\delta = -519$) and $PI_4^+SbF_6^-$ ($\delta = -517$), which is due to spin–orbit (SO) contributions from the four heavy iodine substituents, transmitted to the phosphorus nucleus by a very effective Fermi-contact mechanism. The less negative solid-state ^{31}P NMR chemical shifts found in the polymeric $PI_4^+AlI_4^-$ ($\delta = -305$) and $PI_4^+GaI_4^-$ ($\delta = -295$), suggest that the P–I bond orders are reduced due to intermolecular I ··· I interaction between PI_4^+ cations and EI_4^- (E = Al, Ga) anions.[6]

PCl_3Br^+, $PCl_2Br_2^+$ and $PClBr_3^+$ have been characterised by ^{31}P NMR and Raman spectroscopy in solids and solutions containing mixtures of the chlorobromophosphonium cations $PCl_nBr_{4-n}^+$ ($0 \le n \le 4$).[3,12] Replacement of a chlorine by a bromine causes an upfield shift of about 40 ppm. Solution-state ^{31}P NMR studies showed that there is a characteristic chemical shift range dependent upon the nature of the counter-ion present. The variation of the ^{31}P chemical shift for $PCl_nBr_{4-n}^+$ ($0 \le n \le 4$) as a function of the anion in the solid-state is even larger.[3] The mixed chloroiodophosphonium cations PCl_3I^+ and $PCl_2I_2^+$ formed from the reaction of PI_3 with the strongly acidic solvent $HSClO_3$ were characterised by means of solution-state ^{31}P NMR spectroscopy.[13]

To our knowledge, prior to this study there had been no evidence for the existence of the mixed tetrahalophosphonium cations $PBr_nI_{4-n}^+$ ($1 \le n \le 3$). Only the existence of the PBr_3I^+ cation has been assumed in the reaction of PBr_3 and I_2 in acetic anhydride in a conductivity study.[14]

In this paper we report the preparation and characterisation of a complete series of the mixed bromoiodophosphonium cations by means of solid-state ^{31}P MAS NMR spectroscopy. To allow unequivocal assignment, we have computed the ^{31}P NMR chemical shifts of the free cations $PBr_nI_{4-n}^+$ ($0 \le n \le 4$) by density functional theory (DFT) methods corrected for SO coupling. The results of the ^{31}P MAS NMR and the vibrational spectra clearly indicate that the counter-ion has a dramatic influence on the chemical shift and the vibrational frequencies of the tetrahalophosphonium species. Additionally, $PI_4^+AlCl_4^-$, $PI_4^+AlBr_4^-$ and $PI_4^+GaI_4^-$ have been structurally characterised by single-crystal X-ray diffraction.

Results and discussion

Synthesis

Tetrabromophosphonium hexafluoroarsenate, $PBr_4^+AsF_6^-$, was prepared by the reaction of one equivalent of PBr_3 with one equivalent of $Br_3^+AsF_6^-$, reaction 1, eqn. 1, in $CFCl_3$.

$$PBr_3 + Br_3^+AsF_6^- \xrightarrow{CFCl_3} PBr_4^+AsF_6^- + Br_2 \qquad (1)$$

The colourless product formed was characterised by solid-state ^{31}P MAS NMR and vibrational spectroscopy. Additionally, we recorded the solid-state ^{31}P MAS NMR spectra of $PBr_4^+AlBr_4^-$ and $PBr_4^+GaBr_4^-$, which were prepared according to the literature.[2e] $PI_4^+AlBr_4^-$ and $PI_4^+GaBr_4^-$ were prepared from the reaction of PI_3 with IBr and EBr_3 (reactions 2 and 3, E = Al, Ga) in a 1 : 1 : 1 molar ratio, eqn. 2, in CS_2 under nitrogen.

$$PI_3 + IBr + EBr_3 \xrightarrow{CS_2} PI_4^+EBr_4^- \qquad (2)$$

† Crystal structure analyses.

 DOI: 10.1039/b101197i

Table 1 MP2-optimised bond distances [Å] and bond angles [°] for the tetrahalophosphonium cations $PBr_nI_{4-n}^+$ ($0 \le n \le 4$) compared to experimental values

	PBr_4^{+a}	In $PBr_4^+Br^{-b}$	PBr_3I^+	$PBr_2I_2^+$	$PBrI_3^+$	PI_4^{+a}	In $PI_4^+AlCl_4^{-c}$	In $PI_4^+AlBr_4^{-d}$	In $PI_4^+GaI_4^{-e}$
Point group	T_d		C_{3v}	C_{2v}	C_{3v}	T_d			
P–Br	2.153	2.13(3)–2.17(3)	2.162	2.171	2.177				
P–I			2.399	2.407	2.415	2.423	2.361(4)–2.372(4)	2.376(3)–2.387(4)	2.378(4)–2.423(4)
Br–P–Br	109.5	107.9(16)–110.0(10)	108.6	107.7					
Br–P–I			110.4	109.4	108.6				
I–P–I				111.4	110.4	109.5	108.8(2)–110.5(2)	107.4(1)–112.0(1)	106.9(1)–112.6(2)

[a] See ref. 6. [b] See ref. 9. [c] See Table 4. [d] See Table 2. [e] See Table 3.

Solid-state ^{31}P and ^{71}Ga MAS NMR studies (see below) showed that for $PI_4^+GaBr_4^-$ the tetrabromogallate(III) anion is partly substituted by mixed bromoiodogallate anions, arising from a halogen exchange during the preparation.

Tetraiodophosphonium tetrachloroaluminate, $PI_4^+AlCl_4^-$ was obtained from the reaction of PI_3 with ICl and $AlCl_3$ in a 1 : 1 : 1 molar ratio, reaction 4, eqn. 3, in CS_2.

$$PI_3 + ICl + AlCl_3 \xrightarrow{CS_2} PI_4^+AlCl_4^- \qquad (3)$$

The synthesis of pure compounds containing the mixed bromoiodophosphonium ions is extremely difficult. Attempts to prepare pure PBr_3I^+ species were unsuccessful. Initial preparations involving reactions of PBr_3 with $I_3^+MF_6^-$ (reactions 5 and 6, M = As, Sb) in $CFCl_3$ or PBr_3 with IBr and EBr_3 (reactions 7 and 8, E = Al, Ga) in CS_2, led to products which were obviously mixtures of $PBr_nI_{4-n}^+$.

All products reported here exist only in the solid-state. Dissolving *e.g.* $PI_4^+AlBr_4^-$ in CS_2 gives a solution that contains essentially the starting materials, while $PBr_4^+AsF_6^-$ is not soluble in common solvents.

Structures

The P–X distances and X–P–X angles for the isolated tetrahalophosphonium cations $PBr_nI_{4-n}^+$ ($0 \le n \le 4$), computed at the MP2 level of theory, are summarised in Table 1. The results for PBr_4^+ and PI_4^+ agree very well with the available X-ray data.

The unit cell of $PI_4^+AlBr_4^-$ is shown in Fig. 1, selected bond lengths and angles are listed in Table 2. $PI_4^+AlBr_4^-$ crystallises in the monoclinic space group $P2_1/c$ with four molecules in the unit cell. The PI_4^+ unit has a considerably distorted tetrahedral geometry. The P–I bonds are almost equal: 2.376(3)–2.387(4) Å, the I–P–I bond angles range between 107.4(1) and 112.0(1)°. The $AlBr_4^-$ anion is also significantly distorted exhibiting bond angles between 107.3(2) and 116.8(5)° and Al–Br distances between 2.290(5) and 2.314(4) Å, which are comparable with the bond lengths found in $SeBr_3^+AlBr_4^-$.[15]

$PI_4^+GaI_4^-$ (Fig. 2, Table 3) crystallises in the orthorhombic space group $Pna2_1$ with four molecules in the unit cell. The structure is isotypic with $PI_4^+AlI_4^-$.[11] The tetrahedra of the cations and anions are significantly distorted, exhibiting I–E–I angles between 106.9(1) and 112.6(1)° (PI_4^+) and between 107.12(6) and 112.90(5)° (GaI_4^-). P–I distances vary from 2.378(4) to 2.423(4) Å, Ga–I distances from 2.510(1) to 2.573(2) Å. P–I bond lengths and I–P–I bond angles are comparable to those found in $PI_4^+AlI_4^-$.[11]

The average P–I bond length of $PI_4^+AlBr_4^-$ (2.381(4) Å) is significantly shorter than the average P–I bond length found in $PI_4^+GaI_4^-$ (2.408(4) Å). Similar to $PI_4^+AlI_4^-$ the molecular structure of $PI_4^+GaI_4^-$ shows rather short interatomic I ··· I distances in the range of 3.357(2)–3.430(2) Å (Fig. 2) between the PI_4^+ and the GaI_4^- units, which are significantly shorter than the sum of the van der Waals radii (*ca.* 4.30 Å),[16] indicating strong cation ··· anion interactions, while the crystal structure of $PI_4^+AlBr_4^-$ shows considerably weaker interatomic I ··· Br contacts of 3.380(2)–3.449(2) Å (sum of van der Waals radii: *ca.* 4.10 Å,[16] Fig. 1).

The crystal structure of $PI_4^+AlCl_4^-$ (Fig. 3, Table 4), which is isotypic with $PI_4^+AlBr_4^-$, displays a more isolated character for PI_4^+ in this species, exhibiting rather short P–I bond distances (2.361(4)–2.371(4) Å), significantly diminished interatomic I ··· Cl distances (3.315(8)–3.511(3) Å, sum of van der Waals radii: *ca.* 3.95 Å)[16] and a less distorted tetrahedral geometry (108.8(2)–110.5(2)°) compared to the structures of $PI_4^+GaI_4^-$ and $PI_4^+AlBr_4^-$.

Table 2 Selected bond lengths [Å] and angles [°] for $PI_4^+AlBr_4^-$

P–I(1)	2.380(4)	Al–Br(1)	2.290(5)
P–I(2)	2.387(4)	Al–Br(2B)	2.30(1)
P–I(3)	2.381(4)	Al–Br(3)	2.314(4)
P–I(4)	2.376(3)	Al–Br(4)	2.312(5)
I(1)–P–I(2)	109.4(2)	Br(1)–Al–Br(2B)	116.8(5)
I(1)–P–I(3)	112.0(1)	Br(1)–Al–Br(3)	108.0(2)
I(1)–P–I(4)	109.5(1)	Br(1)–Al–Br(4)	108.0(2)
I(2)–P–I(3)	107.4(1)	Br(2B)–Al–Br(3)	108.1(7)
I(2)–P–I(4)	110.6(1)	Br(2B)–Al–Br(4)	108.3(3)
I(3)–P–I(4)	107.9(2)	Br(3)–Al–Br(4)	107.3(2)

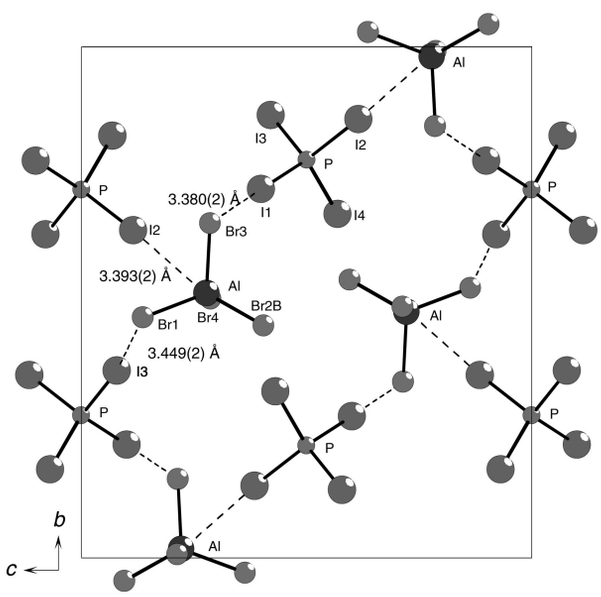

Fig. 1 Unit cell of $PI_4^+AlBr_4^-$.

Table 3 Selected bond lengths [Å] and angles [°] for $PI_4^+GaI_4^-$

P–I(1)	2.416(4)	Ga–I(5)	2.573(2)
P–I(2)	2.423(4)	Ga–I(6)	2.510(2)
P–I(3)	2.414(3)	Ga–I(7)	2.359(2)
P–I(4)	2.378(4)	Ga–I(8)	2.548(2)
I(1)–P–I(2)	106.9(1)	I(5)–Ga–I(6)	112.90(5)
I(1)–P–I(3)	112.6(1)	I(5)–Ga–I(7)	107.60(6)
I(1)–P–I(4)	110.0(1)	I(5)–Ga–I(8)	107.12(6)
I(2)–P–I(3)	110.5(1)	I(6)–Ga–I(7)	111.83(6)
I(2)–P–I(4)	108.8(1)	I(6)–Ga–I(8)	108.69(6)
I(3)–P–I(4)	108.0(1)	I(7)–Ga–I(8)	108.50(6)

Table 4 Selected bond lengths [Å] and angles [°] for $PI_4^+AlCl_4^-$

P–I(1)	2.367(4)	Al–Cl(1)	2.129(6)
P–I(2)	2.372(4)	Al–Cl(2)	2.144(6)
P–I(3)	2.371(4)	Al–Cl(3B)	2.18(4)
P–I(4)	2.361(4)	Al–Cl(4B)	2.05(4)
I(1)–P–I(2)	110.1(2)	Cl(1)–Al–Cl(2)	106.8(2)
I(1)–P–I(3)	110.0(2)	Cl(1)–Al–Cl(3B)	105(1)
I(1)–P–I(4)	108.8(2)	Cl(1)–Al–Cl(4B)	127(2)
I(2)–P–I(3)	109.1(2)	Cl(2)–Al–Cl(3B)	112(1)
I(2)–P–I(4)	110.5(2)	Cl(2)–Al–Cl(4B)	107.8(6)
I(3)–P–I(4)	108.4(2)	Cl(3B)–Al–Cl(4B)	104(2)

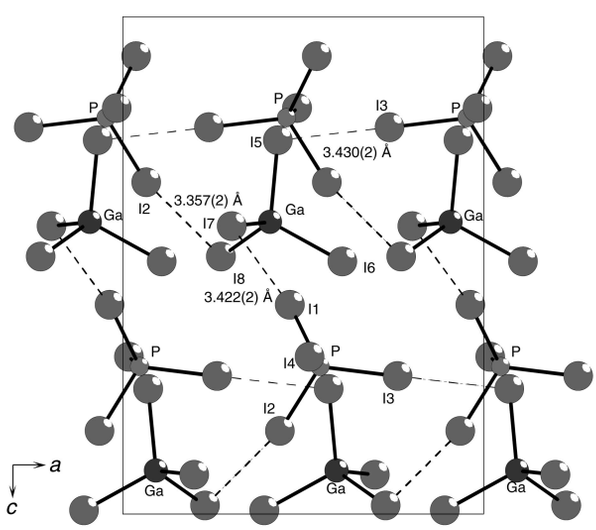

Fig. 2 Unit cell of $PI_4^+GaI_4^-$.

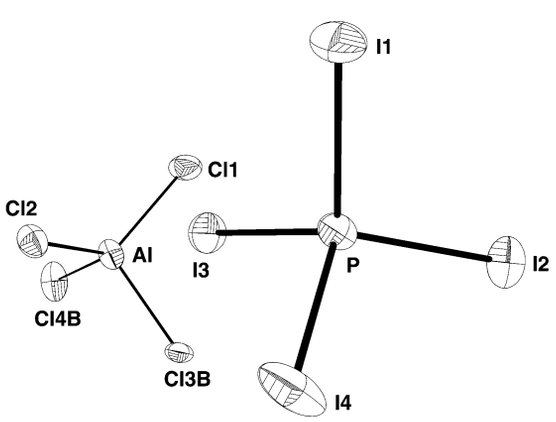

Fig. 3 Molecular structure of $PI_4^+AlCl_4^-$.

Solid-state ^{31}P NMR spectroscopy

PX_4^+ salts. The solid obtained by the reaction of PBr_3 and $Br_3^+AsF_6^-$ (reaction 1, Table 5) gives a ^{31}P MAS NMR spectrum consisting of a single resonance of chemical shift −83 ppm. The ^{31}P chemical shift agrees with literature values reported for PBr_4^+ compounds ($\delta = -72$ to -80)[3] and can be assigned as $PBr_4^+AsF_6^-$. As expected,[6] the comparison with the ^{31}P MAS NMR chemical shifts of $PBr_4^+AlBr_4^-$ ($\delta = -79$) and $PBr_4^+GaBr_4^-$ ($\delta = -80$) shows that the chemical shift of $PBr_4^+AsF_6^-$ is slightly shifted to low frequency, due to the non-coordinating character of the counter-ion.

The ^{31}P MAS NMR spectrum of $PI_4^+AlBr_4^-$ (reaction 2, Table 5, Fig. 4) shows one single resonance at $\delta = -416$, and is in the range between the isotropic shifts of the polymeric $PI_4^+GaI_4^-$ ($\delta = -295$) and the isolated $PI_4^+AsF_6^-$ ($\delta = -519$).[6] This appears consistent with the molecular structure of $PI_4^+AlBr_4^-$, which might also be described as intermediate between these two extremes.

The ^{31}P MAS NMR spectrum of the product of reaction 3 (PI_3/IBr/$GaBr_3$, Table 5, Fig. 5) shows one main signal at $\delta = -387$ (rel. int. 65%), which can be attributed to the isotropic shift of $PI_4^+GaBr_4^-$, as well as four other less intense resonances at $\delta = -376$ (rel. int. 18%), −358 (rel. int. 10%), −344 (rel. int. 2%) and −312 (rel. int. 5%).

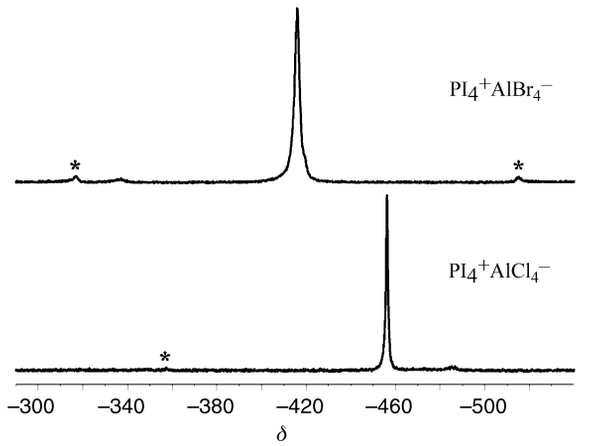

Fig. 4 MAS solid-state ^{31}P NMR spectra of $PI_4^+AlBr_4^-$ and $PI_4^+AlCl_4^-$ at a spinning frequency of 20 kHz. Asterisks denote spinning side bands.

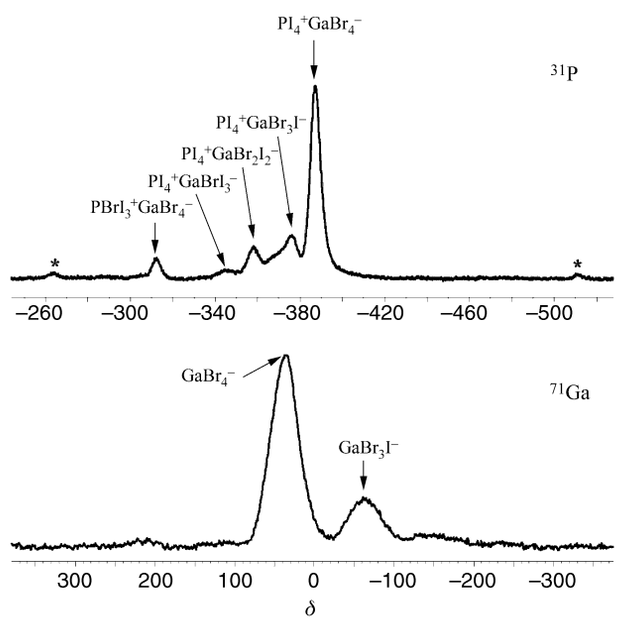

Fig. 5 MAS solid-state ^{31}P and ^{71}Ga NMR spectra for reaction 3 (PI_3 + IBr + $GaBr_3$) at a spinning frequency of 25 and 27 kHz, respectively. The isotropic chemical shifts are indicated by arrows. Asterisks denote spinning side bands.

Table 5 ^{31}P NMR isotropic chemical shifts [ppm *vs.* 85% H_3PO_4] for reactions 1–8

	Reaction		δ	Rel. intensity [%]	ω_{rot}/kHz	Assignment
1	$PBr_3 + Br_3^+AsF_6^-$	^{31}P	−83	100	25	$PBr_4^+AsF_6^-$
2	$PI_3 + IBr + AlBr_3$	^{31}P	−416	100	20	$PI_4^+AlBr_4^-$
3	$PI_3 + IBr + GaBr_3$	^{31}P	−312	5	25	$PBrI_3^+GaBr_4^-$
			−344	2		$PI_4^+GaBrI_3^-$
			−358	10		$PI_4^+GaBr_2I_2^-$
			−376	18		$PI_4^+GaBr_3I^-$
			−387	65		$PI_4^+GaBr_4^-$
		^{71}Ga	37	78	27	$GaBr_4^-$
			−64	22		$GaBrI_3^-$
4	$PI_3 + ICl + AlCl_3$	^{31}P	−456	100	20	$PI_4^+AlCl_4^-$
5	$PBr_3 + I_3^+AsF_6^-$	^{31}P	−83	81	25	$PBr_4^+AsF_6^-$
			−195	17		$PBr_3I^+AsF_6^-$
			−315	2		$PBr_2I_2^+AsF_6^-$
6	$PBr_3 + I_3^+SbF_6^-$	^{31}P	−33	11	25	$PF_4^+SbF_6^-$
			−81	85		$PBr_4^+SbF_6^-$
			−196	4		$PBr_3I^+SbF_6^-$
7	$PBr_3 + IBr + AlBr_3$	^{31}P	−79	46	30	$PBr_4^+AlBr_4^-$
			−167/−171	35		$PBr_3I^+AlBr_4^-$
			−250	16		$PBr_2I_2^+AlBr_4^-$
			−331	3		$PBrI_3^+AlBr_4^-$
8	$PBr_3 + IBr + GaBr_3$	^{31}P	−68	2	30	$PBr_4^+GaBrI_3^-$
			−74	6		$PBr_4^+GaBr_2I_2^-$
			−78	5		$PBr_4^+GaBr_3I^-$
			−80	34		$PBr_4^+GaBr_4^-$
			−155	6		$PBr_3I^+GaBr_3I^-$
			−170	35		$PBr_3I^+GaBr_4^-$
			−254	12		$PBr_2I_2^+GaBr_4^-$

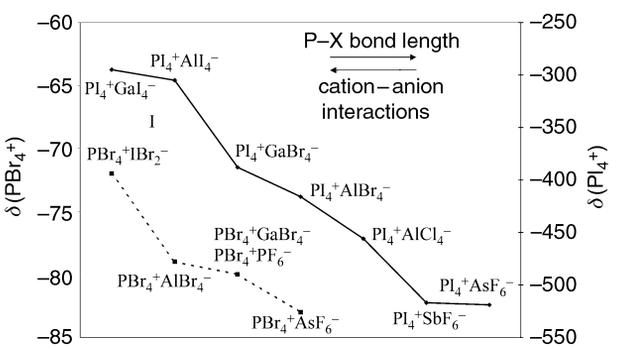

Fig. 6 ^{31}P NMR chemical shifts for some PBr_4^+ and PI_4^+ species.

Fig. 6 summarises the ^{31}P NMR chemical shifts of some PBr_4^+ and PI_4^+ species in the presence of different counter-anions. The chemical shift of PX_4^+ is dependent on the nature of the counter-anion. Significant bridging cation ··· anion interactions in the lattice result in a weakening of the P–X bonds in PX_4^+. The comparison of the crystal structures of $PI_4^+AlCl_4^-$, $PI_4^+AlBr_4^-$ and $PI_4^+GaI_4^-$ show a more isolated character for the PI_4^+ cations in $PI_4^+AlCl_4^-$ and $PI_4^+AlBr_4^-$ with weaker interatomic cation ··· anion interactions and considerably shorter P–I bond lengths than found in $PI_4^+GaI_4^-$. The more isolated the cation, the more efficient is the Fermi-contact mechanism that transfers the SO-induced spin density to the ^{31}P nucleus.[17] The ^{31}P resonance is shifted to low frequency.[6] In case of the PBr_4^+ cation the chemical shift range is very small and varies from $\delta = -72$ to -83. In contrast, for PI_4^+ species the anion has a significant influence. Due to much larger spin–orbit effects,[6] the ^{31}P chemical shift for PI_4^+ salts varies over a considerably larger range, between $\delta = -295$ ($PI_4^+GaI_4^-$) and -519 ($PI_4^+AsF_6^-$). Thus, it is possible to take the low frequency ^{31}P chemical shift as a measure of the intermolecular interactions. For mixed $PI_4^+EBr_nI_{4-n}^-$ ($0 \le n \le 4$) species it is expected that a gradual replacement of bromine by iodine in the counter-anion causes a trend towards high frequency for the ^{31}P chemical shift of PI_4^+.

The ^{31}P MAS NMR spectrum of the product of reaction 3 clearly indicates that halogen exchange resulting in a partial substitution of the $GaBr_4^-$ by mixed tetrahalogenogallate(III) anions has occurred during the reaction. The resonances at $\delta = -376$, -358 and -344 with a decreasing relative intensity can be attributed to the chemical shifts of $PI_4^+GaBr_3I^-$, $PI_4^+GaBr_2I_2^-$ and $PI_4^+GaBrI_3^-$. Moreover, the presence of different tetrahalogenogallate(III) anions in the solid obtained by reaction 3 was confirmed by solid-state ^{71}Ga MAS NMR spectroscopy. The ^{71}Ga MAS NMR spectrum (Fig. 5, Table 5) at a spinning frequency of 27 kHz reveals two broad resonances centred at $\delta = 37$ (rel. int. 78%) and -64 (rel. int. 22%). The ^{71}Ga isotropic chemical shifts for the two resonances are comparable with the previous results of the solution-state ^{71}Ga NMR studies for $GaBr_nI_{4-n}^-$ and can be assigned to the resonances of $GaBr_4^-$ (δ ^{71}Ga = 37 in the solid-state; δ ^{71}Ga = 65 in solution)[18] and $GaBr_3I^-$ (δ ^{71}Ga = −64 in the solid-state; δ ^{71}Ga = −48 in solution).[18] The expected less intense signals for $GaBr_2I_2^-$ (δ ^{71}Ga = −173 in solution)[18] and $GaBrI_3^-$ (δ ^{71}Ga = −309 in solution)[18] at higher field could not be resolved due to the large linewidths of the ^{71}Ga resonances and overlapping spinning side bands. Similar halogen exchange mechanisms were reported in recent ^{71}Ga NMR studies on ligand-exchange reactions between GaX_4^- and GaY_4^- (X, Y = Cl, Br, I). The ^{71}Ga chemical shifts for all possible four-coordinate gallates GaX_4^- (X = Cl, Br, I) and mixed-halide species $GaX_nY_{4-n}^-$ (X, Y = Cl, Br, I) were found.[18] Note that the low frequency shift with increasing number of iodine substituents is also due to SO effects.[19] The impurity at $\delta = -312$ in the ^{31}P NMR spectra of reaction 3 may be attributed to the resonance of $PBrI_3^+GaBr_4^-$.

The ^{31}P NMR chemical shift of $\delta = -456$ found for $PI_4^+AlCl_4^-$ (Fig. 4, Table 5, reaction 4) is at lower frequency, as compared to $PI_4^+EX_4^-$ (E = Al, Ga; X = Br, I). This suggests that the PI_4^+ cation in $PI_4^+AlCl_4^-$ has a more isolated character and smaller I ··· Cl interactions in the solid-state, which is in agreement with the crystal structure.

Reaction products containing mixtures of $PBr_nI_{4-n}^+$. Density functional calculations of the ^{31}P chemical shifts in isolated $PBr_nI_{4-n}^+$ (Table 6, Fig. 7) show the significant influence of SO effects. While the non-relativistic calculations would predict a slight increase in δ ^{31}P from PBr_4^+ through PI_4^+, SO

Table 6 Comparison of computed and experimental ^{31}P shifts [ppm *vs.* 85% H_3PO_4]

	δ_{NR} [b]	δ_{SO} [c]	δ_{NR+SO} [d]	Exp. [e]	[f]	[g]	[h]	[i]	[j]	[k]
PBr_4^+ [a]	179	−205	−26	−83	−81		−79	−80		
PBr_3I^+	197	−317	−120	−196	−195		−167	−170		
$PBr_2I_2^+$	207	−415	−208	−315			−250	−254		
$PBrI_3^+$	212	−588	−376				−331	−312		
PI_4^+ [a]	211	−734	−523	−519[a]	−517[a]	−456	−416	−387	−305[a]	−295[a]

[a] See ref. 6. [b] Non-relativistic DFT calculation. [c] One- and two-electron spin–orbit corrections. [d] Spin–orbit corrected result. [e] AsF_6^- salts. [f] SbF_6^- salts. [g] $AlCl_4^-$ salt. [h] $AlBr_4^-$ salts. [i] $GaBr_4^-$ salts. [j] AlI_4^- salt. [k] GaI_4^- salt.

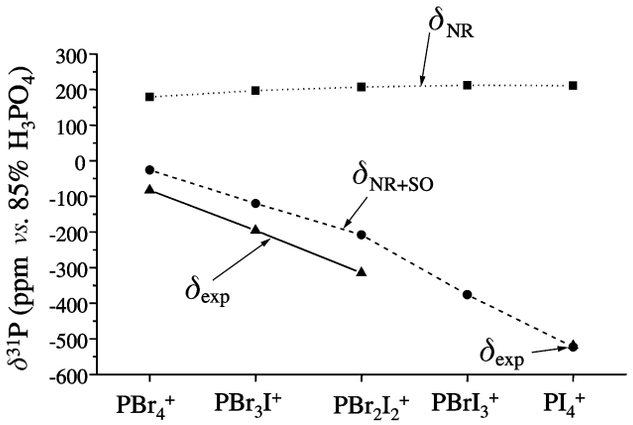

Fig. 7 Comparison of the computed and experimental isotropic ^{31}P shifts (data from Table 6). Dotted line: non-relativistic calculations; dashed line: results with one- and two-electron SO corrections; solid line: experimental data.

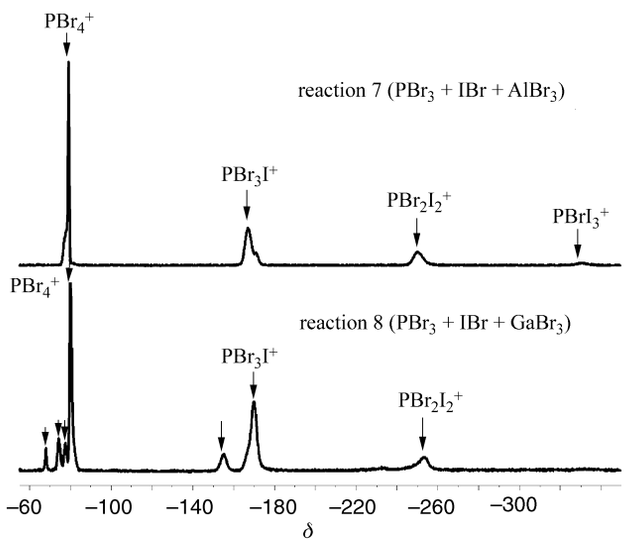

Fig. 8 MAS solid-state ^{31}P NMR spectrum for reaction 7 (PBr_3/IBr/$AlBr_3$) and reaction 8 (PBr_3/IBr/$GaBr_3$) at a spinning frequency of 30 kHz. The isotropic chemical shifts are indicated by arrows.

contributions increase from δ −205 to −734 and thus are responsible for the observed large low frequency shifts upon increasing substitution by iodine.[6] Based on these computational results for the isolated cations, we assigned the experimentally observed resonances found in the ^{31}P NMR spectra of the solids formed by reactions 5 to 8.

Products from reactions 5 and 6 are clearly mixtures of PBr_4^+ and PBr_3I^+ species ($PBr_4^+AsF_6^-$: $\delta = -83$; $PBr_4^+SbF_6^-$: $\delta = -81$; $PBr_3I^+AsF_6^-$: $\delta = -195$; $PBr_3I^+SbF_6^-$: $\delta = -196$). A small amount of formed $PBr_2I_2^+AsF_6^-$ could be detected as a broad resonance at $\delta = -315$ in the ^{31}P MAS NMR spectrum of reaction 5 (Table 5). An additional peak at $\delta = -33$ in the ^{31}P MAS NMR spectrum of reaction 6 corresponds with literature values of the ^{31}P chemical shift for the PF_4^+ cation and indicates that a partial fluorination at phosphorus has obviously occurred during the reaction.[1c]

The ^{31}P MAS NMR spectrum of the solid yielded by the PBr_3/IBr/$AlBr_3$ reaction system (reaction 7) at 30 kHz (Fig. 8, Table 5) indicates the existence of all considered mixed bromoiodophosphonium complexes. The main signal at $\delta = -79$ can be assigned as $PBr_4^+AlBr_4^-$. The two resonances found at $\delta = -167$ and −171 represent the ^{31}P chemical shifts for PBr_3I^+ species. The weak and broad lines at $\delta = -250$ and −331 can be allocated to the ^{31}P MAS NMR chemical shifts for the $PBr_2I_2^+$ and $PBrI_3^+$ tetrabromoaluminate(III) salts, respectively.

The ^{31}P MAS NMR spectrum of the solid obtained from reaction 8 (PBr_3/IBr/$GaBr_3$) at 30 kHz (Fig. 8, Table 5) indicates that in this mixture there are four, two and one resonances associated with the PBr_4^+, PBr_3I^+ and $PBr_2I_2^+$ regions, respectively. This suggests that a similar halogen exchange as found for reaction 3 has occurred during the preparation. Besides the signal for $PBr_4^+GaBr_4^-$ at $\delta = -80$ three narrow lines appear at higher frequency which can be attributed to the signals of $PBr_4^+GaBr_3I^-$ ($\delta = -78$), $PBr_4^+GaBr_2I_2^-$ ($\delta = -74$ ppm), and $PBr_4^+GaBrI_3^-$ ($\delta = -68$). The ^{31}P resonance at $\delta = -170$ displays the same value as assigned for $PBr_3I^+AlBr_4^-$ and can be allocated to $PBr_3I^+GaBr_4^-$. The weaker resonance at $\delta = -153$ ppm may be attributed to $PBr_3I^+GaBr_3I^-$. The resonance at $\delta = -254$ is close to that observed for $PBr_2I_2^+AlBr_4^-$ and can be assigned to $PBr_2I_2^+GaBr_4^-$.

In most cases, the AsF_6^- and SbF_6^- salts are thought to be representative of "ideal" ionic species, whereas for EX_4^- (E = Al, Ga; X = Br, I) salts non-negligible interactions between complex cations and anions have to be considered. On average the low frequency shift from PBr_4^+ to PI_4^+ increases in intervals of roughly 85 ppm for $AlBr_4^-$. In contrast, the increasing tendency to lower frequency of the ^{31}P resonances of the AsF_6^- species from PBr_4^+ to PBr_3I^+ (112 ppm) and from PBr_3I^+ to $PBr_2I_2^+$ (120 ppm) is significantly higher.

Vibrational spectroscopy

$PBr_4^+AsF_6^-$. The Raman spectrum of $PBr_4^+AsF_6^-$ is shown in Fig. 9. The vibrational frequencies and their assignment in comparison with $PBr_4^+EBr_4^-$ (E = Al, Ga) and the computed normal modes for PBr_4^+ are summarised in Table 7.[4c] The frequencies of the PBr_4^+ cation are fairly consistent with literature values. The Raman-active symmetric ν_1 (A_1) stretching mode of the PX_4^+ species is a characteristic frequency to indicate the extent of intermolecular cation ··· anion interactions. The ν_1 (A_1) stretching mode at 266 cm^{-1} in $PBr_4^+AsF_6^-$ is at considerably higher frequency than in $PBr_4^+EBr_4^-$ (E = Al: 256 cm^{-1}, Ga: 258 cm^{-1}).[4c] This is consistent with the well-known non-coordinating character of AsF_6^- anions, and with the expectation that no significant interactions between cations and anions occur for this system. A similar phenomenon is reported for the $(i\text{-Pr})_3PI^+$ cation. The P–I stretching vibration of $(i\text{-Pr})_3PI^+SbF_6^-$ at 157 cm^{-1} is raised to higher wavenumbers than found in $(i\text{-Pr})_3PI^+I^-$ (ν (P–I): 150 cm^{-1}) and

Table 7 Calculated and observed fundamental frequencies [cm^{-1}] for PBr_4^+

PBr_4^+ calculation [a]	$PBr_4^+AsF_6^-$ Raman	IR	$PBr_4^+AlBr_4^-$ Raman [b]	IR	$PBr_4^+GaBr_4^-$ Raman [b]	IR	Assignment
511 (126)	512 (8)	513 s	512 sh/510 (4)/500 (5)	515/490	505 (4, br)	510 s	ν_3 (T_2, PBr_4^+)
263 (0)	266 (100)		256 (100)	264 m	258 (100)	250 w	ν_1 (A_1, PBr_4^+)
150 (1)	153 (66)		150 (43)	145 vs	153 sh/150 (50)	155 m	ν_4 (T_2, PBr_4^+)
90 (0)	106 (34)		104 (11)	98 w	104 (23)	108 m	ν_2 (E, PBr_4^+)
	307 (13)						$2 \times \nu_4$ (T_2, PBr_4^+)
	701 (4)	697 vs					ν_3 (T_{1u}, AsF_6^-)
	675 (28)	676 m					ν_1 (A_{1g}, AsF_6^-)
	577 (5)	580 w					ν_2 (E_g, AsF_6^-)
		391 s					ν_4 (T_{1u}, AsF_6^-)
	368 (61)						ν_5 (T_{2g}, AsF_6^-)

[a] IR intensity [km mol^{-1}] in parentheses. [b] See ref. 4*c*.

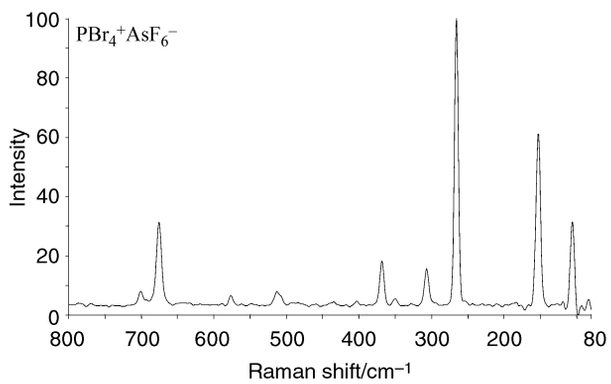

Fig. 9 Raman spectrum of $PBr_4^+AsF_6^-$.

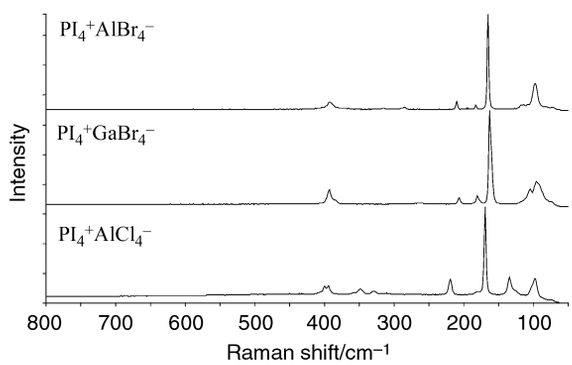

Fig. 10 Raman spectra of $PI_4^+AlBr_4^-$, $PI_4^+GaBr_4^-$ and $PI_4^+AlCl_4^-$.

in $(i\text{-Pr})_3PI^+I_3^-$ (ν (P–I): 148 cm^{-1}), due to shorter P–I distances and less pronounced intermolecular interactions.[20]

The IR spectrum of $PBr_4^+AsF_6^-$ shows two expected IR active modes, ν_3 (T_{1u}) and ν_4 (T_{1u}), at 697 and 391 cm^{-1} for a free AsF_6^- anion, which are consistent with literature values.[21] The Raman active ν_1 (A_{1g}), ν_2 (E_g) and ν_5 (T_{2g}) modes for AsF_6^- were observed at 675, 577 and 368 cm^{-1}. The appearance of two absorptions at 676 and 580 cm^{-1} in the IR spectrum of $PBr_4^+AsF_6^-$, which can be assigned to the ν_1 (A_{1g}) and ν_2 (E_g) modes of AsF_6^-, leads to the conclusion that the octahedral symmetry of the anion in $PBr_4^+AsF_6^-$ may be slightly distorted.

$PI_4^+EBr_4^-$ (E = Al, Ga). The solid-state Raman spectra of $PI_4^+EBr_4^-$ (E = Al, Ga) and $PI_4^+AlCl_4^-$ are shown in Fig. 10. The computed and experimentally observed vibrational frequencies and their assignments are summarised in Table 8 in comparison with the vibrational frequencies found for $PI_4^+EI_4^-$ (E = Al, Ga) and $PI_4^+MF_6^-$ (M = As, Sb).

The symmetric ν_1 (A_1) stretching mode for the anions in $PI_4^+EBr_4^-$ (E = Al, Ga) can be observed as the most intense peaks in the Raman spectra at 165 (E = Al) and 163 cm^{-1} (E = Ga), respectively. When compared with the vibrational spectra of $PI_4^+EI_4^-$ (E = Al, Ga), the ν_1 (A_1) stretching mode is significantly shifted to higher frequencies (12–14 cm^{-1}). In contrast to these results, the ν_1 (A_1) stretching mode was found close to 194 cm^{-1} in $PI_4^+MF_6^-$ (M = As, Sb).[5] This appears consistent with the suggestion that the vibration frequencies should be at lower wavenumbers, because the P–I bond order in the compounds $PI_4^+EBr_4^-$ (E = Al, Ga) is reduced by weak I ··· Br cation ··· anion interactions, whereas the PI_4^+ cation in $PI_4^+MF_6^-$ (M = As, Sb) is almost isolated.

The presence of the anions EBr_4^- (E = Al, Ga) is confirmed by the symmetric stretching mode, ν_1 (A_1), at 210 cm^{-1} ($PI_4^+AlBr_4^-$) and 207 cm^{-1} ($PI_4^+GaBr_4^-$). They are consistent with literature values (ν_1 ($AlBr_4^-$): 212 cm^{-1};[22] ν_1 ($GaBr_4^-$): 210 cm^{-1} [23]). The strong absorptions in the IR spectra at 393 cm^{-1} ($PI_4^+AlBr_4^-$) and 263 cm^{-1} ($PI_4^+GaBr_4^-$) can be assigned to the antisymmetric stretching mode, ν_3 (T_2), of EBr_4^-. Confirmed by the results of the ^{31}P and ^{71}Ga MAS NMR data, the sample of reaction 3 was a mixture of mostly $PI_4^+GaBr_4^-$ and small amounts of $PI_4^+EBr_nI_{4-n}^-$. Two intense bands at 278 and 240 cm^{-1} in the IR spectrum of $PI_4^+GaBr_4^-$ can be assigned to stretching vibrations of the partially replaced $GaBr_3I^-$ anion. Both Raman spectra of $PI_4^+EBr_4^-$ (E = Al, Ga) exhibit weak peaks at *ca.* 182 cm^{-1} due to small I_2 impurities.

Consistent with the ^{31}P MAS NMR results the experimentally observed symmetric P–I [ν_1 (A_1)] stretching mode of the more isolated salt $PI_4^+AlCl_4^-$ at 169 cm^{-1} appears at considerably higher wavenumbers than found in the complexes $PI_4^+EX_4^-$ (E = Al, Ga; X = Br, I). The Raman and IR frequencies at 496 (ν_3), 350 (ν_1), 219 (ν_4) and 134 cm^{-1} (ν_2) agree with literature values[2c] reported for the fundamental frequencies of $AlCl_4^-$ and confirm the presence of this counter-anion.

Reaction products containing mixtures of $PBr_nI_{4-n}^+$. The solids formed from reactions 5 to 8 gave very complex IR and Raman spectra. Assignment of the fundamental frequencies of the mixed bromoiodophosphonium complexes is consequently very difficult. Besides the frequencies for PBr_4^+, the fundamental modes for the anions AsF_6^- (reaction 5), SbF_6^- (reaction 6), $AlBr_4^-$ (reaction 7) and $GaBr_4^-$ (reaction 8) were found in the vibrational spectra. With respect to the computed vibrational frequencies and the results of the ^{31}P MAS NMR data, we attempted to assign the fundamental frequencies of the PBr_3I^+ cation in a reasonable way, as summarised in Table 9.

The Raman active stretching mode, ν_1 (A_1), can be observed as intense peaks at 240 (AsF_6^-, reaction 5), 237 (SbF_6^-, reaction 6) and 222 ($GaBr_4^-$, reaction 8) cm^{-1} in the Raman spectra. As expected, significant increases in frequency occur for all modes of the PBr_3I^+ cation on passing from complexes where tetrahaloaluminate and tetrahalogallate anions are present to those with the anions AsF_6^- and SbF_6^-.

Table 8 Calculated and observed fundamental frequencies [cm^{-1}] for PI_4^+

PI_4^+ calculation[a]	$PI_4^+AsF_6^-$ Raman[b]	IR	$PI_4^+AlCl_4^-$ Raman	IR	$PI_4^+AlBr_4^-$ Raman	IR	$PI_4^+GaBr_4^-$ Raman[c]	IR	$PI_4^+AlI_4^-$ Raman[b]	IR	$PI_4^+GaI_4^-$ Raman[b,d]	IR	Assignment
405 (69)			400 (17)/ 394 (17)	399 vs	392 (16, br)	393 vs, br	393(17)	390 s	380 (20)	380br	378 (20)	382 m/ 375 m	ν_3 (T_2, PI_4^+)
173 (0)	193 (100)		169 (100)		165 (100)		163 (100)		152 (100)		151 (100)		ν_1 (A_1, PI_4^+)
99 (0)	89 (35)		98 (25)		98 (44)		95 (26)		95 (20)		94 (20)		ν_4 (T_2, PI_4^+)
65 (0)	71 (60)				71 (3)		74 (3)		77 (5)		72 (5)		ν_2 (E, PI_4^+)
		697 s											ν_3 (T_{1u}, MF_6^-)
		392 s											ν_4 (T_{1u}, MF_6^-)
				496 s, br	392 (16, br)	393 vs, br	263 (3)	263 vs	321 (5)	329 br	211 (5)	234 s/ 223 vs	ν_3 (T_2, EX_4^-)
			350 (14)	354 w	210 (11)	207 w	207 (9)	207 w	149 (40)		147 (30)		ν_1 (A_1, EX_4^-)
			219 (24)	219 m	114 (11)		105 (18)						ν_4 (T_2, EX_4^-)
			134 (26)		98 (44)		74 (3)						ν_2 (E, EX_4^-)

[a] IR intensity [km mol^{-1}] in parentheses. [b] See ref. 5. [c] $GaBr_4^-$ anions are partially replaced by $GaBr_3I^-$. Two intense IR absorptions assigned to the stretching vibrations of the $GaBr_3I^-$ anion were observed at 278 and 240 cm^{-1}. [d] See ref. 6.

Conclusion

The solid-state ^{31}P MAS NMR studies for PI_4^+ species show extremely large negative ^{31}P isotropic shifts ranging from $\delta = -295$ to -519. They depend considerably on the nature of the counter-ion. The more isolated the character of the PI_4^+ cation (shorter P–I bond lengths, weaker cation ··· anion interactions), the larger the P–I bond order becomes. Consequently, the Fermi-contact mechanism that transfers the spin–orbit induced spin density to the phosphorus nucleus is more efficient,[17] and the ^{31}P resonance is shifted to higher field.[6] Significant donor–acceptor contacts between cation and anion in the solid-state lead to less pronounced low frequency isotropic ^{31}P shifts. Additionally, a trend towards higher wavenumbers for the fundamental frequencies of PI_4^+ could be observed from the polymeric $[PI_4^+EI_4^-$ (E = Al, Ga)] to the "ideal" ionic cases $[PI_4^+MF_6^-$ (M = As, Sb)]. For PBr_4^+ species these effects are less pronounced.

Based on the results of the computed isotropic ^{31}P chemical shifts for isolated $PBr_nI_{4-n}^+$ cations, we found evidence for the existence of the hitherto unknown mixed bromoiodophosphonium cations PBr_3I^+, $PBr_2I_2^+$ and $PBrI_3^+$ by means of solid-state ^{31}P MAS NMR spectroscopy.

Due to increasing spin–orbit effects, the δ ^{31}P shifts of the EBr_4^- salts (E = Al, Ga) move increasingly to low frequency along the series $PBr_4^+ < PBr_3I^+ < PBr_2I_2^+ < PBrI_3^+ < PI_4^+$, in intervals of about 85 ppm. In the case of MF_6^- counter-anions (M = As, Sb), the corresponding increments to low frequency are significantly larger, due to the essentially isolated nature of the cations.

Experimental

General methods

All compounds reported here are moisture sensitive. Consequently, strictly anaerobic and anhydrous conditions were employed for their synthesis. Any subsequent manipulations were carried out inside a glove-box under dry nitrogen. $AlBr_3$, $AlCl_3$, Br_2, $GaBr_3$, IBr, ICl, I_2, PBr_3 and PI_3 (all Aldrich) were used as received. $PBr_4^+AlBr_4^-$,[4c] $PBr_4^+GaBr_4^-$[4c] and $PI_4^+GaI_4^-$[6] were prepared according to the literature. The preparation of $Br_3^+AsF_6^-$,[24] $I_3^+AsF_6^-$[25] and $I_3^+SbF_6^-$[26] also followed literature procedures. $CFCl_3$ and CS_2 were refluxed with P_4O_{10} and distilled before used.

^{31}P and ^{71}Ga NMR spectra were measured at 202.49 and 152.48 MHz, respectively, with a BRUKER DSX AVANCE 500 FT NMR spectrometer under fast spinning conditions about the magic-angle (MAS). A standard double-bearing MAS probe designed for zirconia dioxide rotors (diameter: 2.5 mm) was used with spinning frequencies up to 30 kHz. For the ^{31}P NMR measurements a single pulse acquisition was used and the 90° pulse length was adjusted to 2.0 μs. The recycle delay was set to values between 5 and 60 s, depending on the spin lattice relaxation time, to ensure correct relative signal intensities.

For the ^{71}Ga NMR measurements a 16-fold phase cycled Hahn echo sequence (90°–t_1–180°–t_1–acquisition) was used. The interpulse distance t_1 was set to the inverse spinning frequency ($t_1 = 1/\nu_{rot} = 1/27$ kHz). The 90° (1.6 μs) and 180° (3.1 ns) pulses were adjusted to maximal signal intensity.

Due to fast spinning conditions ($\nu_{rot} > 20$ kHz), the recorded spectra contain only few spinning side bands which are clearly separated from the isotropic chemical shift resonances. Therefore, the values for the isotropic chemical shifts of the cations under study could be extracted directly from the spectra without simulations taking into account the chemical shift anisotropy. Overlapping signals were deconvoluted using a pseudo-Voigt profile. The samples were filled under a nitrogen atmosphere in a glove-box. The ^{31}P spectra were referenced to

85% H_3PO_4 in $CDCl_3$, isotropic ^{71}Ga chemical shifts to an external 1.0 M solution of $Ga(NO_3)_3$.

Raman spectra were obtained of powdered solid samples contained in glass capillary tubes with a Perkin-Elmer 2000 NIR spectrometer in the range 800–50 cm^{-1}. IR spectra were recorded on Nujol mulls between CsI plates in the range 800–200 cm^{-1} on a Nicolet 520 FT IR spectrometer. For the determination of decomposition points, samples were heated in sealed glass capillaries in a Büchi B450 instrument.

Syntheses

Reaction 1: preparation of $PBr_4^+AsF_6^-$. PBr_3 (0.61 g, 2.25 mmol) was reacted with $Br_3^+AsF_6^-$ (0.97 g, 2.25 mmol) in $CFCl_3$ (15 mL) with stirring at room temperature in a two-bulbed glass vessel incorporating a coarse sintered-glass frit and a Young valve. An intense brown solution of Br_2 over a colourless solid was obtained. After stirring for 2 h the solution was filtered. Solvent and traces of remaining Br_2 were removed under dynamic vacuum, leaving a colourless solid. Yield: 0.35 g (29%), mp 144–148 °C (decomp.).

Reaction 2: preparation of $PI_4^+AlBr_4^-$. PI_3 (0.41 g, 1.00 mmol) was reacted with IBr (0.20 g, 1.00 mmol) and $AlBr_3$ (0.27 g, 1.00 mmol) in CS_2 (20 mL) with stirring at room temperature. After stirring for 2 h the solvent was removed under dynamic vacuum, leaving a red solid. Yield: 0.82 g (93%), mp 109 °C (decomp.).

Reaction 3 (PI_3 + IBr + $GaBr_3$). PI_3 (0.41 g, 1.00 mmol) was reacted with IBr (0.20 g, 1.00 mmol) and $GaBr_3$ (0.31 g, 1.00 mmol) in CS_2 (20 mL) with stirring at room temperature. After stirring for 2 h the solvent were removed under dynamic vacuum, leaving a red solid. Yield: 0.79 g, mp 86 °C (decomp.).

Reaction 4: preparation of $PI_4^+AlCl_4^-$. PI_3 (0.82 g, 2.00 mmol) was reacted with ICl (0.32 g, 2.00 mmol) and $AlCl_3$ (0.27 g, 2.00 mmol) in CS_2 (30 mL) with stirring at room temperature. After stirring for 2 h the solvent and traces of ICl were removed at 50 °C under dynamic vacuum, leaving an orange solid. Yield: 0.97 g (69%), mp 70 °C (decomp.).

Reaction 5 (PBr_3 + $I_3^+AsF_6^-$). PBr_3 (0.27 g, 1.00 mmol) was reacted with $I_3^+AsF_6^-$ (0.57 g, 1.00 mmol) in $CFCl_3$ (15 mL) with stirring at room temperature in a two-bulbed glass vessel incorporating a coarse sintered-glass frit and a Young valve. An intense dark purple solution over a pale brownish solid was obtained. After stirring for 24 h the solution was filtered, and refiltered several times, by condensing about half the solvent back and refiltering. Solvent and traces of remaining I_2 were removed under dynamic vacuum, leaving a pale brownish solid. Yield: 0.31 g, mp 146 °C (decomp.).

Reaction 6 (PBr_3 + $I_3^+SbF_6^-$). PBr_3 (1.04 g, 3.84 mmol) was reacted with $I_3^+SbF_6^-$ (2.37 g, 3.84 mmol) in $CFCl_3$ (20 mL) with stirring at room temperature in a two-bulbed glass vessel incorporating a coarse sintered-glass frit and a Young valve. An intense dark purple solution over a pale brownish solid was obtained. After stirring for 24 h the solution was filtered, and refiltered several times, by condensing about half the solvent back and refiltering. Solvent and traces of remaining I_2 were removed under dynamic vacuum, leaving a pale brownish solid. Yield: 1.25 g, mp 90 °C (decomp.).

Reaction 7 (PBr_3 + IBr + $AlBr_3$). PBr_3 (0.27 g, 1.00 mmol) was reacted with IBr (0.20 g, 1.00 mmol) and $AlBr_3$ (0.27 g, 1.00 mmol) in CS_2 (20 mL) with stirring at room temperature. After stirring for 2 h the solvent was removed under dynamic vacuum, leaving a brown solid. Yield: 0.51 g, mp 97 °C (decomp.).

Reaction 8 (PBr_3 + IBr + $GaBr_3$). PBr_3 (0.27 g, 1.00 mmol) was reacted with IBr (0.20 g, 1.00 mmol) and $AlBr_3$ (0.31 g, 1.00 mmol) in CS_2 (20 mL) with stirring at room temperature. After stirring for 2 h the solvent was removed under dynamic vacuum, leaving an orange solid. Yield: 0.59 g, mp 67–69 °C (decomp.).

Crystallography

Single crystals of $PI_4^+AlCl_4^-$, $PI_4^+AlBr_4^-$ and $PI_4^+GaI_4^-$ suitable for X-ray structure determination were grown from CS_2 and covered with perfluoropolyether oil. The selected crystals were mounted on the tip of a glass fibre and placed on a goniometer head.

Crystal data for $PI_4^+AlCl_4^-$. $AlCl_4I_4P$, $M = 707.35$, monoclinic, $a = 6.523(6)$, $b = 15.81(1)$, $c = 14.34(1)$ Å, $\beta = 92.09(1)°$, $U = 1478(2)$ Å^3, $T = 193(2)$ K, space group $P2_1/c$, $Z = 4$. Siemens CCD area detector, scan type: hemisphere, μ(Mo-Kα, $\lambda = 0.71073$ Å) = 9.277 mm^{-1}, reflections collected: 5309, independent reflections: 1627 ($R_{int} = 0.0308$), observed reflections: 1292 [$F > 4\sigma(F)$]. Absorption correction: SADABS.[27] Structure solution and refinement program: SHELXL-97,[28] direct methods, final R indices for all atoms in anisotropic description [$F > 4\sigma(F)$]: $R1 = 0.0440$, $wR2 = 0.1023$, $R1 = 0.0613$, $wR2 = 0.1099$ (all data).

Crystal data for $PI_4^+AlBr_4^-$. $AlBr_4I_4P$, $M = 885.19$, monoclinic, $a = 6.6475(8)$, $b = 16.471(2)$, $c = 14.534(4)$ Å, $\beta = 91.832(2)°$, $U = 1590.5(3)$ Å^3, $T = 188(2)$ K, space group $P2_1/c$, $Z = 4$. Siemens CCD area detector, scan type: hemisphere, μ(Mo-Kα, $\lambda = 0.71073$ Å) = 17.996 mm^{-1}, reflections collected: 6541, independent reflections: 2056 ($R_{int} = 0.0374$), observed reflections: 1673 [$F > 4\sigma(F)$]. Absorption correction: SADABS.[27] Structure solution and refinement program: SHELXL-97,[28] direct methods, final R indices for all atoms in anisotropic description [$F > 4\sigma(F)$]: $R1 = 0.0447$, $wR2 = 0.1080$, $R1 = 0.0580$, $wR2 = 0.1145$ (all data).

Crystal data for $PI_4^+GaI_4^-$. GaI_8P, $M = 1115.89$, orthorhombic, $a = 11.0101(7)$, $b = 10.4007(7)$, $c = 15.1835(9)$ Å, $U = 1738.7(2)$ Å^3, $T = 200(2)$ K, space group $Pna2_1$, $Z = 4$. Stoe IPDS diffractometer, μ(Mo-Kα, $\lambda = 0.71073$ Å) = 15.839 mm^{-1}, reflections collected: 9490, independent reflections: 3879 ($R_{int} = 0.0257$), observed reflections: 3142 [$F > 2\sigma(I)$]. Absorption correction: numerical. Structure solution and refinement program: SHELXL-97,[28] direct methods, final R indices for all atoms in anisotropic description [$F > 2\sigma(I)$]: $R1 = 0.0377$, $wR2 = 0.0758$, $R1 = 0.0516$, $wR2 = 0.0785$ (all data).

CCDC reference numbers 158050–158052.

See http://www.rsc.org/suppdata/dt/b1/b101197i/ for crystallographic data in CIF or other electronic format.

Computational methods

The structures of the isolated $PBr_nI_{4-n}^+$ ($0 \le n \le 4$) were optimised at the second-order Møller–Plesset (MP2) level with the program package Gaussian 98.[29] Quasirelativistic pseudopotentials and DZP valence basis sets were employed for P, I, and Br.[30] All species were characterised as minima by harmonic vibrational frequency analysis.[31] It should be noted that the calculations were performed on isolated (gas-phase) cations. There may well be significant differences between gas-phase and solid-state data.

The DFT calculations of ^{31}P chemical shifts were carried out at the same theoretical level as in ref. 6. The initial, non-relativistic nuclear shielding calculations (uncorrected for spin–orbit coupling) used the sum-over-states density functional perturbation theory approach (SOS-DFPT),[32,33] with individual gauges for localised orbitals (IGLO[34]). The

Table 9 Calculated and observed fundamental frequencies [cm^{-1}] for PBr_3I^+

PBr_3I^+ calculation[a]	PBr_3/I_3AsF_6 Reaction 5 Raman	IR	PBr_3/I_3SbF_6 Reaction 6 Raman	IR	$PBr_3/IBr/AlBr_3$ Reaction 7 [b] IR	$PBr_3/IBr/GaBr_3$ Reaction 8 Raman	IR	Assignment
497 (108)		498 m		497 m	486 m	486 (5)	482 m	ν_4 (A_1, PBr_3I^+)
462 (119)		466 m		464 m	456 m	452 (6)	447 m	ν_2 (E, PBr_3I^+)
237 (1)	240 (25)	242 w	237 (100)	239 w	226 m	223 (100)	222 m	ν_1 (A_1, PBr_3I^+)
139 (1)	141 (16)					138 (39)		ν_3 (E, PBr_3I^+)
132 (1)	136 (17)					124 (47)		ν_6 (A_1, PBr_3I^+)
88 (0)								ν_5 (E, PBr_3I^+)

[a] IR intensity [km mol^{-1}] in parentheses. [b] The Raman spectrum of the product showed fluorescence and therefore no Raman data was available.

underlying Kohn–Sham calculations employed the gradient-corrected PW91[35] exchange-correlation functional. All calculations were carried out with the deMon-KS[36] and deMon-NMR[32] codes.

IGLO-II all-electron basis sets[34] were used on all atoms (omitting f-functions on iodine due to program limitations), with density and exchange-correlation potential fitting auxiliary basis sets of the sizes 5,4 (P) and 5,5 (Br, I) (*n*,*m* denotes *n* s-functions and *m* spd-shells with shared exponents[36]). All six Cartesian components of d-basis functions were kept. The IGLO procedure[34] employed the Boys localisation scheme.[37] For comparison to experiment, the computed absolute shieldings σ were converted to relative shifts δ *via* the absolute shielding value of 328.4 ppm for 85% H_3PO_4 given by Jameson *et al.*[38]

Spin–orbit corrections to the nuclear shieldings were computed separately by the combined finite-perturbation/SOS-DFPT ansatz of ref. 32. A recently implemented and validated[39] mean field approximation was used to compute the one- and two-electron SO integrals. An IGLO choice of gauge origin has been used in the calculation of the SO corrections. The calculations of the spin–orbit corrections used the same basis sets described above, but the spherical d-basis functions were projected out for compatibility with the SO integral code. 64 points of radial quadrature and the PP86 functional[40] were employed. The initial finite perturbation (with a perturbation parameter $\lambda = 10^{-5}$ arbitrary units) was chosen to be the nuclear magnetic moment of the phosphorus nucleus.

Acknowledgements

We gratefully acknowledge the support of the Fonds der Chemischen Industrie and the University of Munich. In addition we would like to thank Prof. Peter N. Gates and Prof. Günther Engelhardt, Dr Axel Schulz and Dipl.-Chem. Gernot Kramer for valuable discussions and Andrea Barra for NMR spectroscopic measurements. M.K. is grateful to Deutsche Forschungsgemeinschaft for support (Schwerpunktprogramm "Relativistische Effekte") and thanks Dr Vladimir G. Malkin and Dr Olga L. Malkina for helpful discussions.

References

1 (*a*) G. S. H. Chen and J. Passmore, *J. Chem. Soc., Chem. Commun.*, 1973, 559; (*b*) G. S. H. Chen and J. Passmore, *J. Chem. Soc., Dalton Trans.*, 1979, 1251; (*c*) R. Minkwitz and A. Liedtke, *Z. Naturforsch., Teil B*, 1989, **44**, 679.
2 (*a*) J. Shamir, S. Luski, S. Cohen and D. Gibson, *Inorg. Chem.*, 1985, **24**, 2301; (*b*) P. N. Gates, H. C. Knachel, A. Finch, A. V. Fratini and A. N. Fitch, *J. Chem. Soc., Chem. Commun.*, 1995, 2719; (*c*) P. Reich and H. Preiss, *Z. Chem.*, 1967, **7**, 115; (*d*) R. Rafaeloff and J. Shamir, *Spectrochim. Acta, Part A*, 1974, **30**, 1305; (*e*) J. Shamir, B. J. van der Kehlen, M. A. Herman and R. Rafaeloff, *J. Raman Spectrosc.*, 1981, **11**, 215; (*f*) W. Wieker and A.-R. Grimmer, *Z. Naturforsch., Teil B*, 1967, **22**, 257; (*g*) W. Wieker and A.-R. Grimmer, *Z. Naturforsch., Teil B*, 1966, **21**, 1103; (*h*) A. Finch, P. N. Gates and A. S. Muir, *J. Chem. Res. (S)*, 1986, 68.
3 K. B. Dillon, R. K. Harris, P. N. Gates, A. S. Muir and A. Root, *Spectrochim. Acta, Part A*, 1991, **47**, 831.
4 (*a*) W. Gabes and H. Gerding, *Recueil*, 1971, **90**, 157; (*b*) W. Gabes, K. Olie and H. Gerding, *Recueil*, 1972, **91**, 1367; (*c*) J. Shamir, S. Schneider and B. J. van der Kehlen, *J. Raman Spectrosc.*, 1986, **17**, 463.
5 I. Tornieporth-Oetting and T. M. Klapötke, *J. Chem. Soc., Chem. Commun.*, 1990, 132.
6 M. Kaupp, Ch. Aubauer, G. Engelhardt, T. M. Klapötke and O. L. Malkina, *J. Chem. Phys.*, 1999, **110**, 3687.
7 Ch. Aubauer, T. M. Klapötke and A. Schulz, *Int. J. Vibr. Spectrosc.*, 1999, **3**, 4 (http://www.ijvs.com/volume3/edition2/section4.htm).
8 (*a*) H. Preiss, *Z. Anorg. Allg. Chem.*, 1971, **380**, 51; (*b*) H. Preiss, *Z. Anorg. Allg. Chem.*, 1971, **380**, 56; (*c*) W. F. Zelezny and N. C. Baenzinger, *J. Am. Chem. Soc.*, 1952, **74**, 6151; (*d*) D. Clark, H. M. Powell and A. F. Wells, *J. Chem. Soc.*, 1942, 642; (*e*) J. C. Taylor and A. B. Waugh, *Polyhedron*, 1983, **2**, 211; (*f*) J. Shamir, S. Schneider, A. Bino and S. Cohen, *Inorg. Chim. Acta*, 1986, **114**, 35; (*g*) J. Shamir, S. Schneider, A. Bino and S. Cohen, *Inorg. Chim. Acta*, 1986, **114**, 141; (*h*) C. F. Erdbrügger, P. G. Jones, R. Schelbach, E. Schwarzmann and G. M. Sheldrick, *Acta Crystallogr., Sect. C*, 1987, **43**, 1857; (*i*) H. Preut, D. Lennhoff and R. Minkwitz, *Acta Crystallogr., Sect. C*, 1992, **48**, 1648; (*j*) M. L. Ziegler, B. Nuber, K. Weidenhammer and G. Hoch, *Z. Naturforsch., Teil B*, 1977, **32**, 18; (*k*) P. H. Collins and M. Webster, *Acta Crystallogr., Sect. B*, 1972, **28**, 1260; (*l*) B. Krebs, B. Buss and W. Berger, *Z. Anorg. Allg. Chem.*, 1973, **397**, 1; (*m*) T. J. Kistenmacher and G. D. Stucky, *Inorg. Chem.*, 1968, **7**, 2150; (*n*) T. J. Kistenmacher and G. D. Stucky, *Inorg. Chem.*, 1971, **10**, 122; (*o*) A. Finch, A. N. Fitch and P. N. Gates, *J. Chem. Soc., Chem. Commun.*, 1993, 957; (*p*) P. N. Gates, H. C. Knachel, A. Finch, A. V. Fratini, A. N. Fitch, O. Nardone, J. C. Otto and D. A. Snider, *J. Chem. Soc., Dalton Trans.*, 1995, 2719; (*q*) B. Neumüller, C: Lau and K. Dehnicke, *Z. Anorg. Allg. Chem.*, 1996, **622**, 1847; (*r*) G. V. Khvorykh, S. I. Troyanov, A. I. Baranov and A. A. Sereov, *Z. Anorg. Allg. Chem.*, 1998, **624**, 1026; (*s*) A. I. Baranov, G. V. Khvorykh and S. I. Troyanov, *Z. Anorg. Allg. Chem.*, 1999, **625**, 1240; (*t*) J. Beck, K. Müller-Buschbaum and F. Wolf, *Z. Anorg. Allg. Chem.*, 1999, **625**, 975.
9 W. Gabes and K. Olie, *Acta Crystallogr., Sect. B*, 1970, **26**, 443.
10 G. L. Breneman and R. D. Willett, *Acta Crystallogr.*, 1967, **23**, 467.
11 S. Pohl, *Z. Anorg. Allg. Chem.*, 1983, **498**, 15.
12 (*a*) A.-R. Grimmer, *Z. Anorg. Allg. Chem.*, 1973, **400**, 105; (*b*) K. B. Dillon and P. N. Gates, *J. Chem. Soc., Chem. Commun.*, 1972, 348; (*c*) A. Finch, P. N. Gates, F. J. Ryan and F. F. Bentley, *J. Chem. Soc., Dalton Trans.*, 1973, 1863; (*d*) K. B. Dillon, M. P. Nisbet and T. C. Waddington, *Inorg. Nucl. Chem. Lett*, 1973, **9**, 63; (*e*) K. B. Dillon and A. W. G. Platt, *Polyhedron*, 1982, **1**, 123; (*f*) K. B. Dillon and A. W. G. Platt, *Polyhedron*, 1983, **2**, 641.
13 K. B. Dillon, M. P. Nisbet and T. C. Waddington, *J. Chem. Soc., Chem. Commun.*, 1979, 883.
14 K. C. Malhotra and D. S. Katoch, *Aust. J. Chem.*, 1975, **28**, 991.
15 J. Beck and A. Fischer, *Z. Anorg. Allg. Chem.*, 1995, **621**, 1042.
16 *Handbook of Chemistry and Physics* , 52nd edn., ed. R. C. Weast, The Chemical Rubber Co., Cleveland, 1971–1972, p. D-146.
17 M. Kaupp, O. L. Malkina, V. G. Malkin and P. Pyykkö, *Chem. Eur. J.*, 1998, **4**, 118.
18 (*a*) B. R. McGarvey, M. J. Taylor and D. G. Tuck, *Inorg. Chem.*, 1981, **20**, 2010; (*b*) R. Coloton, D. Dakternieks and J. Hauenstein, *Aust. J. Chem.*, 1981, **34**, 949.
19 See, *e.g.* H. Takashima, M. Hada and H. Nakatsuji, *Chem. Phys. Lett.*, 1995, **235**, 13.
20 F. Ruthe, P. G. Jones, W.-W. du Mont, P. Deplano and M. L. Mercuri, *Z. Anorg. Allg. Chem.*, 2000, **626**, 1105.
21 T. Birchall, P. A. W. Dean, B. della Valle and R. J. Gillespie, *Can. J. Chem.*, 1953, **51**, 667.

22 G. M. Begun, C. R. Boston, G. Torsi and G. Mamantov, *Inorg. Chem.*, 1971, **10**, 886.
23 L. A. Woodward and A. A. Nord, *J. Chem. Soc.*, 1955, 2655.
24 O. Glemser and A. Smalc, *Angew. Chem.*, 1969, **81**, 531.
25 J. Passmore and P. Taylor, *J. Chem. Soc., Dalton Trans.*, 1976, 804.
26 R. J. Gillespie, M. J. Morton and J. M. Sowa, *Adv. Raman Spectrosc.*, 1972, **1**, 539.
27 G. M. Sheldrick, SADABS, Program for Siemens Area Detector Absorption Correction, University of Göttingen, Germany, 1996.
28 G. M. Sheldrick, SHELXL-97, Program for Crystal Structure Determination, University of Göttingen, Germany, 1997.
29 M. J. Frisch, G. W. Trucks, H. B. Schlegel, G. E. Scuseria, M. A. Robb, J. R. Cheeseman, V. G. Zakrzewski, J. A. Montgomery Jr., R. E. Stratmann, J. C. Burant, S. Dapprich, J. M. Millam, A. D. Daniels, K. N. Kudin, M. C. Strain, O. Farkas, J. Tomasi, V. Barone, M. Cossi, R. Cammi, B. Mennucci, C. Pomelli, C. Adamo, S. Clifford, J. Ochterski, G. A. Petersson, P. Y. Ayala, Q. Cui, K. Morokuma, D. K. Malick, A. D. Rabuck, K. Raghavachari, J. B. Foresman, J. Cioslowski, J. V. Ortiz, B. B. Stefanov, G. Liu, A. Liashenko, P. Piskorz, I. Komaromi, R. Gomperts, R. L. Martin, D. J. Fox, T. Keith, M. A. Al-Laham, C. Y. Peng, A. Nanayakkara, C. Gonzalez, M. Challacombe, P. M. W. Gill, B. Johnson, W. Chen, M. W. Wong, J. L. Andres, C. Gonzalez, M. Head-Gordon, E. S. Replogle and J. A. Pople, Gaussian 98, Revision A.6, Gaussian, Inc., Pittsburgh, PA, 1998.
30 A. Bergner, M. Dolg, W. Kuechle, H. Stoll and H. Preuss, *Mol. Phys.*, 1993, **80**, 1431.
31 D. McQuerrie, *Statistical Mechanics*, Harper & Brown, New York, 1976.
32 V. G. Malkin, O. L. Malkina, L. A. Eriksson and D. R. Salahub, in *Modern Density Functional Theory: A Tool for Chemistry*, ed. J. M. Seminario and P. Politzer, Elsevier, Amsterdam, 1995, vol. 2.
33 V. G. Malkin, O. L. Malkina, M. E. Casida and D. R. Salahub, *J. Am. Chem. Soc.*, 1994, **116**, 5898.
34 W. Kutzelnigg, U. Fleischer and M. Schindler, in *NMR-Basic Principles and Progress*, Springer, Heidelberg, 1990, vol. 23, pp. 165ff.
35 (*a*) J. P. Perdew and Y. Wang, *Phys. Rev. B*, 1992, **45**, 13244; (*b*) J. P. Perdew, in *Electronic Structure of Solids*, ed. P. Ziesche and H. Eischrig, Akademie Verlag, Berlin. 1991; (*c*) J. P. Perdew, J. A. Chevary, S. H. Vosko, K. A. Jackson, M. R. Pederson, D. J. Singh and C. Fiolhais, *Phys. Rev. B*, 1992, **46**, 6671.
36 deMon program: D. R. Salahub, R. Fournier, P. Mlynarski, I. Papai, A. St-Amant and J. Ushio, in *Density Functional Methods in Chemistry*, ed. J. Labanowski and J. Andzelm, Springer, New York, 1991; A. St-Amant and D. R. Salahib, *Chem. Phys. Lett.*, 1990, **169**, 387.
37 (*a*) C. Edmiston and K. Ruedenberg, *Rev. Mod. Phys.*, 1963, **35**, 457; (*b*) C. Edmiston and K. Ruedenberg, *J. Chem. Phys.*, 1965, **43**, 597; (*c*) S. F. Boys, in *Quantum Theory of Atoms, Molecules and the Solid State*, ed. P. O. Löwdin, Academic Press, New York, 1966, pp. 253ff; This procedure is often erroneously attributed to J. M. Foster and S. F. Boys, *Rev. Mod. Phys.*, 1963, **35**, 457.
38 C. J. Jameson, A. de Dios and A. K. Jameson, *Chem. Phys. Lett.*, 1990, **167**, 575.
39 O. L. Malkina, B. Schimmelpfennig, M. Kaupp, B. A. Hess, P. Chandra, U. Wahlgren and V. G. Malkin, *Chem. Phys. Lett.*, 1998, **296**, 93.
40 (*a*) J. P. Perdew, *Phys. Rev. B*, 1986, **33**, 8822; (*b*) J. P. Perdew and Y. Wang, *Phys. Rev. B*, 1986, **33**, 8800.